

# Cross-field plasma lens for focusing of the Hall thruster plume

Martin E Griswold, Yevgeny Raitses and Nathaniel J Fisch

Princeton Plasma Physics Laboratory, Princeton University, Princeton, New Jersey, 08543, USA

E-mail: [martin.griswold@alumni.princeton.edu](mailto:martin.griswold@alumni.princeton.edu)

Received 23 October 2013, revised 7 January 2014

Accepted for publication 17 January 2014

Published 22 July 2014

## Abstract

Hall thrusters produce neutralized ion beams with high current density because the acceleration takes place in quasi-neutral plasma and is not subject to space charge limitation. We tested an external plasma lens (PL) in front of the thruster as a means to focus the thruster plume. In the PL, the plasma is nearly collisionless, with non-magnetized flowing ions and magnetized electrons. Surprisingly, we observed anomalous electron cross-field transport, leading to large currents to the PL electrode and enhanced power loss.

Keywords: Hall thruster, plasma lens, anomalous transport

(Some figures may appear in colour only in the online journal)

## 1. Introduction

Hall thrusters circumvent the space charge limit on current density by accelerating ion beams in quasi-neutral plasma. The acceleration takes place in crossed electric and magnetic fields, with the electric field self-consistently determined by the plasma. The drawback of this arrangement is that it is difficult to optimize the electric field to minimize the divergence of the ion plume. To the extent that the magnetic fields are radial and form equipotential surfaces, the electric fields and hence the acceleration can be axial with small divergence. However, the magnetic fields are not entirely radial, and the field lines do not quite form equipotential surfaces. Although there are phenomena that tend to make these effects cancel in certain variations of the Hall thruster [1], in general there results significant plume divergence. The plume half-angle is about  $45^\circ$  for common thrusters [2] (the plume angle is taken to enclose 90% of the total current). This large divergence can cause problems because high-energy ions at large angles can intersect and damage spacecraft components.

There have been efforts to reduce the plume divergence in Hall thrusters by optimizing the shape of the magnetic field in the thruster channel [3–7], adding ring-shaped electrodes to the channel walls [2, 5], and optimizing the operation of the thruster cathode [8]. However, because the ionization of the gas flow, the acceleration of the ions and the transport of electrons to the anode are all self-organized by the plasma within the channel, it is difficult to optimize ion acceleration without affecting the other processes. Thus, efforts to

reduce the plume divergence can significantly affect the operation of the thruster itself. We sought to de-couple the focusing of the ion beam from its ionization and acceleration using an external plasma lens (PL) to focus the beam after it leaves the channel [9]. The electrostatic PL [10, 11] has a rich heritage in focusing low-divergence, mono-energetic ion beams produced by gridded ion sources [12, 13]. It works by creating a region of crossed electric and magnetic fields using a set of magnetic coils and electrodes on the periphery of the beam. As the beam passes through this region, the ions are accelerated by the electric field so that their trajectories come to a focus downstream of the PL. However, the PL has not previously been applied to Hall thrusters. Hall thrusters have highly divergent plumes with a large spread of ion energy (see figure 6), so the plasma that must be focused by our lens is substantially different than plasmas produced by gridded ion sources: the large beam divergence ( $45^\circ$  for common Hall thrusters [2]) creates sharper density gradients, the ion energy is significantly lower ( $<250$  eV for this work compared with  $>5$  keV for previous PL research [12, 13]) and the non-uniform ion energy causes ion kinetic effects, which are discussed in section 5. The Hall thruster plume, therefore, presents a more difficult target for focusing, but even a modest reduction in the plume divergence would be technologically beneficial.

## 2. Setup

Our setup [9], shown in figure 1, consisted of a PL 10.5–37 cm downstream from a cylindrical Hall thruster (CHT), with a

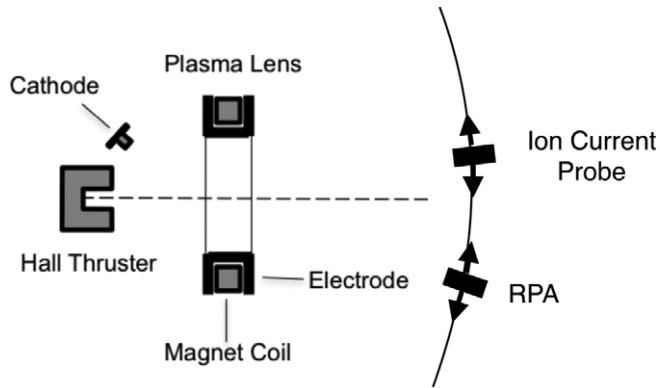


**Figure 1.** Experimental setup. Our setup consisted of a plasma lens downstream of a cylindrical hall thruster. An ion current probe downstream of the PL measured the current density and an RPA measured the ion energy distribution.

guarding ring ‘plume probe’ mounted on a rotating arm that measured ion current in a  $180^\circ$  arc at a radius of 73.2 cm from the thruster channel exit. The thruster operated with a 250 V acceleration voltage and about 0.8 A thruster discharge current. The PL consisted of a single magnet coil enclosed by an electrode. We tested the PL at three different positions,  $D = 10.5, 15.5$  and 37 cm, where  $D$  is the distance from the front of the thruster channel. The PL did not enclose the entirety of the plume current in any of these positions, and in the furthest position only 10% of the total current passed through the center of the PL. This is not optimal for a practical implementation of the PL, but it suffices to demonstrate the principle of operation. The magnet coil in the PL had 223 windings and the PL coil current ranged from 1 to 3 A. The combined magnetic field produced by the thruster magnets and the PL magnet, with 2.5 A PL coil current and the PL located at  $D = 15.5$  cm is shown in figure 2. The field strength at the center of the PL is approximately 40 G. The electrode was biased to a positive voltage in the range 0–125 V with respect to the grounded thruster cathode. The cathode was grounded to get stable operation of the thruster. Larger voltages on the PL were not tested because of the large PL electrode current at these voltages. The PL electrode current is discussed in sections 3 and 6. We measured the plasma potential near the PL using a floating emissive probe on a moveable positioner and we measured ion energy with a retarding potential analyzer (RPA) that was located downstream of the thruster, see figure 1.

### 3. Effect of the PL on thruster operation

The PL focused the plume of the thruster without otherwise altering thruster operation as long as the PL was sufficiently far from the thruster exit and the PL electrode current was sufficiently small. When the PL was in the closest position to the thruster that we tested,  $D = 10.5$  cm (measured from the front of the thruster channel), the PL magnetic field interfered with normal thruster operation. In this position, energizing the PL magnetic field while leaving the PL electrode floating strongly affected thruster operation. The peak ion

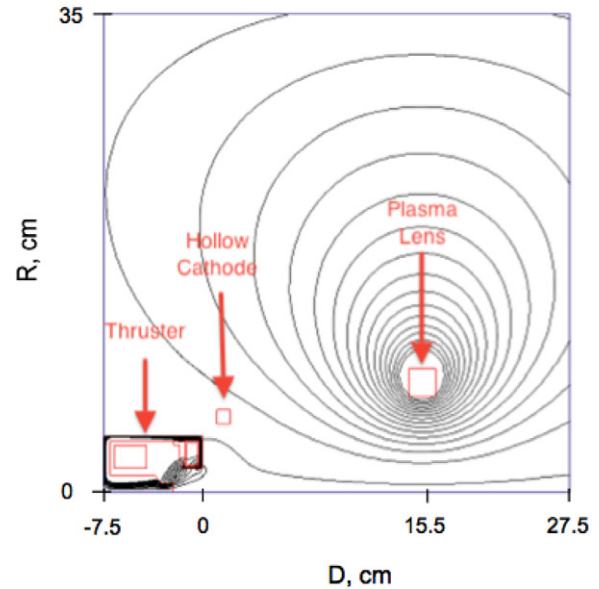


**Figure 2.** Magnetic field of the thruster and plasma lens. The combined magnetic field of the thruster and the PL from finite element simulation. The PL is 15.5 cm downstream from the thruster with 2.5 PL coil current. The field strength at the center of the PL is approximately 40 G.

current density measured by the plume probe dropped by 40% and the discharge current decreased by 12%. This may be because, when the PL is this close to the thruster, its magnetic field alters the field inside the thruster channel or affects the interaction between the thruster channel and the cathode. When the PL was moved further downstream from the thruster (15.5 cm, 37 cm) this effect disappeared and the thruster operated normally.

When the electrode was biased positively with respect to the grounded thruster cathode, the PL electrode current was as large as 2.5 A at 150 V PL electrode positive bias and at the closest position to the thruster,  $D = 10.5$  cm. For the largest PL electrode currents, the thruster discharge current decreased by up to 5%, but for PL electrode current below 1 A, the discharge current was unchanged, suggesting that the thruster operated normally. The thruster discharge current was only 0.8 A, so much of the PL electrode current can be thought of as a discharge between the cathode and the PL electrode. The PL electrode current had a strong dependence on the location of the PL as well as the strength of the PL magnetic field. Figure 3 shows the PL electrode current versus PL electrode voltage for three different positions and with 2 A PL coil current at each position. The PL electrode current decreased as the distance between the thruster and the PL was increased. One possible explanation for this is that the electrode draws less current because the plasma density is lower further out in the plume. If this is the case, it suggests that the PL electrode current at any given axial position could be decreased by increasing the radius of the PL because the plasma density decreases for larger radius. The PL electrode current also had a strong dependence on the magnetic field, decreasing roughly as the inverse of the PL coil current. The electron transport to the PL electrode is discussed further in section 4.

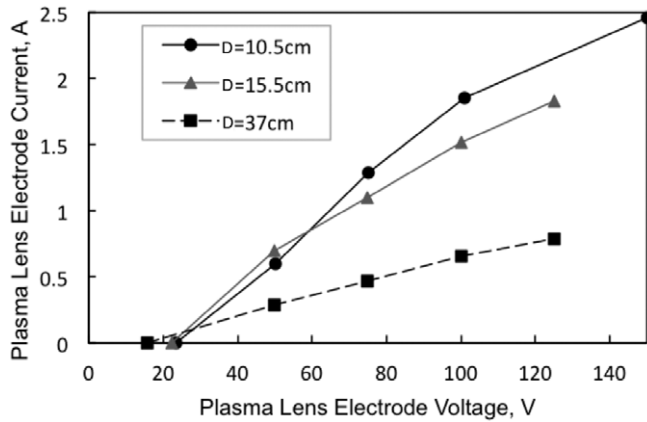


**Figure 3.** Current–voltage plot of the plasma lens electrode. PL electrode current versus PL electrode voltage, for three different PL locations,  $D = 10.5, 15.5$  and  $37$  cm from the thruster exit with  $2$  A PL coil current at each position.

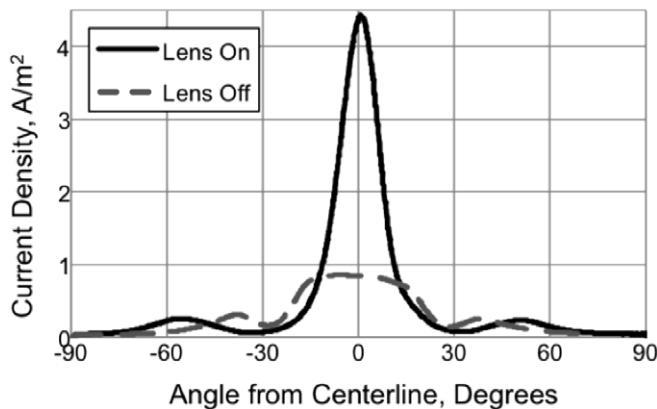


**Figure 4.** Plume current distribution. plume current density versus angle with the PL turned on and off. The PL was considered ‘off’ when there was zero PL coil current and the PL electrode was at its floating voltage of  $+6.4$  V above the grounded thruster cathode. The PL was considered ‘on’ when there was  $2.5$  A PL coil current (field lines shown in figure 2) and  $+100$  V on the PL electrode. These measurements were taken with the PL  $15.5$  cm from the thruster exit.

#### 4. Effect of the PL on the thruster plume

The PL had a large effect on the ion current distribution in the plume, as shown in figure 4. The PL physically obstructs the path of some ions in the plume, and leaves a ‘shadow’ in the ion current density measured by the plume probe (at  $\pm 28^\circ$  and under conditions given in figure 4). This shadow is a useful diagnostic because it marks which portion of the ion current passed through the center of the PL and which portion passed outside. The PL focuses the current that passes through it and it defocuses the current that passes outside. At the PL position  $D = 15.5$  cm,  $2.5$  A PL coil current and  $100$  V on the PL electrode, roughly half (48%) of the total ion current passes through the PL, and this fraction remains constant whether the PL is on or off. With the PL off (i.e. with PL electrode floating and no PL coil current), the 90% half plume angle is  $53.5^\circ$  and the 90% half plume angle for the ‘inside current’ that passes through the PL (current at less than  $\pm 28^\circ$ ) is  $23.8^\circ$ . When the PL is turned on, the half plume angle for the total current

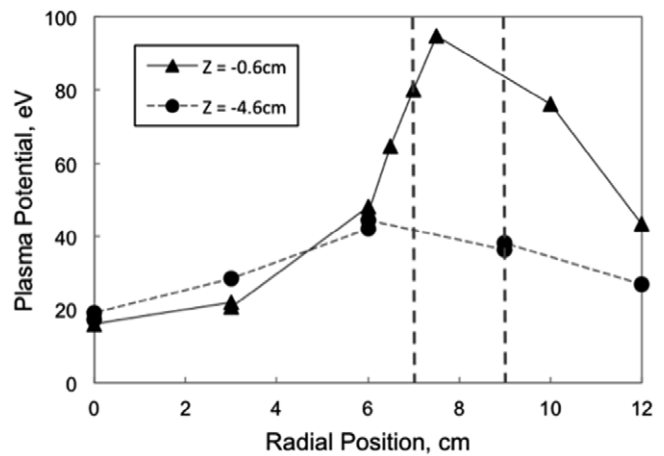


**Figure 5.** Potential drop near the plasma lens. Plasma potential versus radial position, measured along two different axial locations,  $Z$ .  $Z$  is measured from the front of the PL and is negative toward the thruster. Measurements were taken with the PL located  $10.5$  cm from the thruster exit and  $+100$  V on the PL electrode. A floating emissive probe was used to measure the potential. The vertical dashed lines show the radial location of the PL electrode.

increases to  $64.2^\circ$  while the inside current half plume angle decreases to  $19.4^\circ$ . This decrease in the half plume angle for the inside current is not very large. One reason may be that the PL electrode depletes electrons from the plume causing the plume to diverge after the PL due to space charge repulsion. Adding a second cathode after the PL might eliminate this effect.

#### 5. Plasma potential and ion energy measurements

We measured the plasma potential near the PL with a floating emissive probe on a moveable positioner. Because of the constraints of our equipment, measurements were only carried out when the PL was in its closest position to the thruster at  $D = 10.5$  cm. Figure 5 shows the plasma potential versus radial position when the electrode was biased to  $+100$  V. The PL electrode successfully introduces a radial voltage drop of about  $80$  V into the plasma just in front of the PL.

The ion energy distribution, plotted in figure 6, is normalized to the peak value of each curve in order to demonstrate a shift in the average energy. When the PL electrode voltage is increased, the average ion energy measured on the centerline decreases by  $15$  V. This decrease is probably due to an effect involving the energy spread of the ions in the thruster plume. The Hall thruster produces a spread in the ion energy of about  $50$  V, as shown in figure 6. Lower energy ions are more readily influenced by the focusing electric field and will be focused to the center at lower PL electrode voltages than the higher energy ions. Therefore, if the PL electrode voltage is not high enough to bring the higher energy ions to a focus, then more of low energy ions will be measured at the center.

#### 6. Electron transport

The PL electrode current was much larger than we would expect from classical collisions. The collisional current

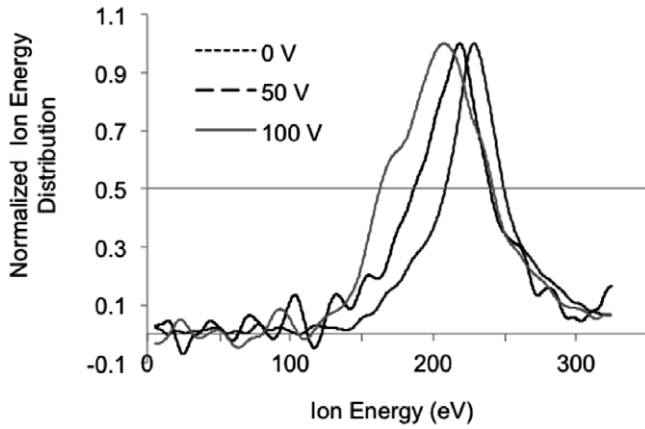


**Figure 6.** Ion energy distribution changes. Ion energy distribution, measured with a retarding potential analyzer downstream of the thruster and PL. For these measurements, the PL coil current was 2.5 A and the IEDF was measured for three settings of the PL electrode voltage: 0, 50 and 100 V.

**Table 1.** Plasma parameters. Parameters near the PL electrode when it is 10.5 cm from the thruster exit with PL electrode voltage of 100 V and PL magnet current of 2 A.  $L_n = (n/\nabla n)$  is the scale length of the density gradient.  $\nu$  is the total collision frequency calculated from the plasma density and the neutral density (calculated from the background pressure of 3  $\mu$  Torr).

$E$	$L_n$	$\nu$	$B$	$n$
35 V/cm	1 cm	26 kHz	25 Gauss	$8.7 \times 10^9 \text{ cm}^{-3}$

density to the PL electrode is calculated from the electron mobility on the last closed field line next to the PL electrode:

$$\mathbf{J} = en\mu_{\perp}\mathbf{E} + eD_{\perp}\nabla n, \quad (1)$$

$$\mu_{\perp} = \frac{e}{m\nu\left(1 + \frac{\omega_c^2}{\nu^2}\right)}, \quad (2)$$

$$D_{\perp} = \frac{kT_e}{m\nu}\left(1 + \frac{\omega_c^2}{\nu^2}\right), \quad (3)$$

where  $\nu$  is the total collision frequency,  $\omega_c = eB/m$  is the cyclotron frequency,  $m$  is the electron mass and  $T_e$  is the electron temperature. We do the calculation using approximate parameters for when the lens is 10.5 cm from the thruster channel exit with 2 A in the PL magnet coil and 100 V on the PL electrode. The parameter values (which err on the side of overestimating the classical current to the PL) are given in table 1.

Using these values in equation (1) gives,  $J_e = 0.12 \text{ A m}^{-2}$ . The total PL electrode current from classical collisions is then found by multiplying  $J_e$  by the area of a toroidal surface enclosing the PL (2 cm minor radius, 16 cm major radius):

$$I = 7 \text{ mA (E)} + 2 \text{ mA (\nabla n)} = 9 \text{ mA}. \quad (4)$$

This accounts for only a small fraction of measured PL electrode current, which was up to 2.5 A, as shown in figure 3. This calculation suggests that anomalous electron transport accounts for much of the PL electrode current. As a point of reference, we calculate the Bohm current. Using the

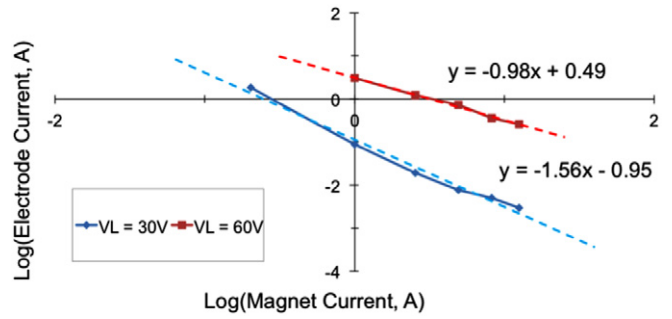


**Figure 7.** Electron transport to the PL versus magnetic field strength plot of the logarithm of the PL electrode current versus the logarithm of the PL coil current (which is proportional to the magnetic field strength) for two different values of the PL electrode voltage. The trend lines show that the electron current to the PL electrode scales as  $B^{-1}$  or  $B^{-1.5}$ . The PL was located at  $D = 105 \text{ cm}$  for these measurements.

parameters from table 1, this gives a value that is much closer to the measured PL electrode current:

$$J_{\text{Bohm}} = \frac{1}{16} \cdot \frac{kT_e}{eB} \quad (5)$$

$$I_{\text{Bohm}} = 2.2 \text{ A}. \quad (6)$$

Furthermore, the PL electrode current does not scale inversely to the square of the magnetic field, as we expect with classical collisions. The scaling was  $B^{-1}$  or  $B^{-1.5}$ , depending on the PL electrode voltage, as is shown in figure 7. This is closer to the Bohm scaling of  $B^{-1}$ . We note that it is not unusual for  $E \times B$  plasma devices to exhibit anomalous electron transport [14], and that oscillations that cause anomalous transport in the thruster channel [15] may contribute to this anomalous transport in the plume.

## 7. Ion shadow diagnostic

While the measurements in figure 4 clearly show that the PL focuses the plume, the plume probe is an imperfect diagnostic. There are several different effects that surely diminish the focus of the plume, but the plume probe data do not shed light on their relative magnitudes. The first effect is that, because of an imperfect potential distribution at the lens, ions traveling at different angles (and therefore arriving to the lens at different radii) might come to a focus at different axial distances downstream. Another effect occurs because the ions are not mono-energetic. Ions travelling along the same initial path, but with different energy will be brought to a different focus. Finally, pressure gradients in the plasma could counteract plasma contraction caused by the PL focusing. Measurements of individual ion trajectories would provide the clearest measure of these effects, but the plume probe only measures the aggregate current density and cannot discern ion trajectories.

We developed a new diagnostic system we call the ‘ion shadow diagnostic’ to measure the approximate trajectories of ions in the plume. The idea was to leverage two existing diagnostic systems to make a new measurement: the Langmuir probe  $r$ - $z$  positioning system and the ion current plume probe.

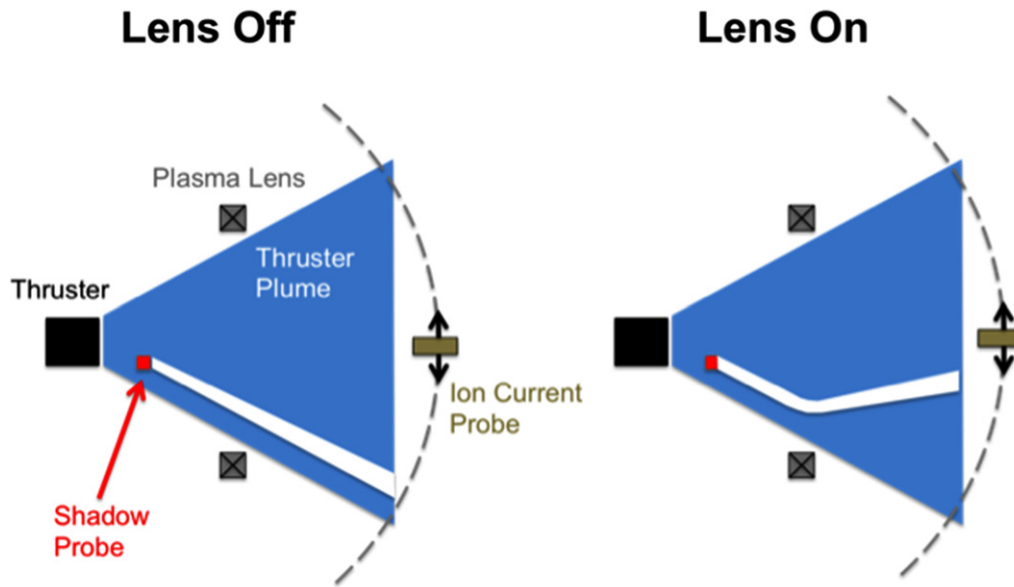


**Figure 8.** Schematic of the ion shadow diagnostic. This method was used to measure approximate ion trajectories in the thruster plume.

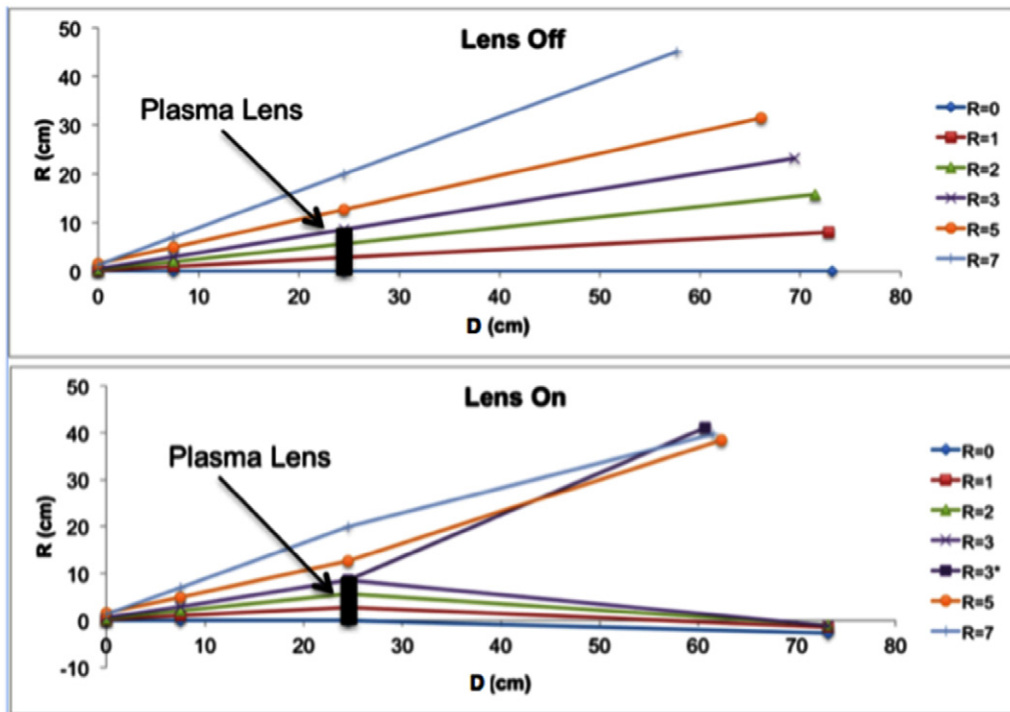


**Figure 9.** Results of the ion shadow diagnostic. The plot shows the approximate ion trajectories that were calculated from the ion shadow diagnostic data. The different  $R$  values refer to the radial position at which the ion trajectory intersects the plane of the PL.

For the new diagnostic, we placed ‘shadow probes’ (strips of carbon paper) on the Langmuir probe positioning system, and moved them in front of the thruster. The purpose of the shadow probes was to physically block the path of some ions, leaving a wake in the plasma flow behind them. This wake would then act as a ‘tracer bullet’ following the trajectory of the ions that surrounded it as it moved through the PL. The wake would show up in the plume probe measurements as a dip in the current density at a certain angular position. By comparing the angular position of the wake measured by the plume probe when the PL was turned off compared to when it was turned

on, we made a 3 point approximation of the ion trajectory (assuming that ions travel in straight lines, with all focusing happening in the plane of the PL). This process is illustrated schematically in figure 8. The results of the measurement are shown in figure 9. They show that the PL brings the average ion to a fairly tight focus.

**8. Discussion and conclusion**

Demonstrating an electrostatic plasma lens in the Hall thruster plume, we showed that it focuses the thruster plume without

otherwise affecting the operation of the thruster. We also identified significant hurdles to the practical application of the PL. The PL electrode consumes 150 W of power, quite large compared with the 200 W consumed in the thruster. Large electron currents to the PL electrode, shown to be anomalous, drive this power loss. It is possible that current transport to the PL electrode could be reduced by increasing the radius of the PL so that it sits in a location where the plasma is less dense, or by moving the cathode to a location that is more magnetically insulated from the PL electrode. These measures to reduce the power loss are likely to increase the weight, making the combined thruster and lens unsuitable for aerospace applications.

However, the combination of the Hall thruster and PL might nonetheless be useful. The results reported here are only a first exploration, neither optimizing the design nor considering different types of Hall thrusters in combination with the PL electrode. The specific thruster on which we tested the PL was the cylindrical Hall thruster (CHT) [16]. This thruster has the advantage that it can naturally be implemented in a cusp mode as well, thereby integrating well with the PL. Although not explored here, this easy integration may be useful in optimizing for reduced combined weight. Similarly, other cusped magnetic field thrusters, such as the DCHT [17] or the DCF [18], which also feature diverging magnetic fields, might similarly lend themselves to optimization in conjunction with an additional lens.

Should these optimizations not prove sufficient to reduce the combined weight of the PL and the thruster for aerospace applications, it may nonetheless be the case that the PL together with a Hall thruster might be useful for terrestrial uses as an industrial ion source [19], where the limitations on power and weight are not as stringent.

## Acknowledgments

This work was supported by the US DOE under Contract No DE-AC02-09CH11466 and by the Air Force Office of Scientific Research. MEG acknowledges the support of a DOE Fusion Energy Sciences Fellowship.

## References

- [1] Fisch N J, Raitses Y and Fruchtman A 2011 Ion acceleration in supersonically rotating magnetized-electron plasma *Plasma Phys. Control. Fusion* **53** 124038
- [2] Raitses Y, Dorf L A, Litvak A A and Fisch N J 2000 Plume reduction in segmented electrode hall thruster *J. Appl. Phys.* **88** 1263–70
- [3] Valentian D, Bugrova A and Morozov A 1993 Development status of the SPT MK II thruster *23rd Int. Electric Propulsion Conf. (Seattle, WA, 13–16 September)* IEPC-93–223
- [4] Hofer R R, Peterson P Y and Gallimore A D 2000 Optimization of Hall thruster magnetic field topography *27th IEEE Int. Conf. on Plasma Science (ICOPS) (New Orleans, LA, 4–7 June)* ICOPS-00-5P02
- [5] Hofer R, Peterson P, Gallimore A and Janovsky R 2001 A high specific impulse two-stage Hall thruster with plasma lens focusing *27th Int. Electric Propulsion Conf. (Pasadena, CA, 15–19 October)* IEPC-01-036
- [6] Fruchtman A and Cohen-Zur A 2006 Plasma lens and plume divergence in the Hall thruster *Appl. Phys. Lett.* **89** 111501
- [7] Cohen-Zur A, Fruchtman A and Gany A 2008 The effect of pressure on the plume divergence in the hall thruster *IEEE Trans. Plasma Sci.* **36** 2069
- [8] Granstedt E M, Raitses Y and Fisch N J 2008 Cathode effects in cylindrical hall thrusters *J. Appl. Phys.* **104** 103302
- [9] Griswold M E, Raitses Y and Fisch N J 2011 Plasma lens focusing of the hall thruster plume *32nd Int. Electric Propulsion Conf. (Wiesbaden, Germany, 11–15 September)* IEPC-2011-177
- [10] Gabor D 1986 A space-charge lens for the focusing of ion beams *Nature* **160** 89–90
- [11] Morozov A I 1965 Focusing of cold quasineutral beams in electromagnetic fields *Dokl. Akad. Nauk SSSR* **163** 1363–6
- [12] Goncharov A A, Zatuagan A V and Protsenko I M 1993 Focusing and control of multiaperture ion beams by plasma lenses *IEEE Trans. Plasma Sci.* **21** 578–81
- [13] Goncharov A A *et al* 1998 Some characteristics of moderate energy metal ion beam focusing by a high current plasma lens *Rev. Sci. Instrum.* **69** 1135–7
- [14] Keidar M and Beilis I I 2006 Electron transport phenomena in plasma devices with  $E \times B$  drift *IEEE Trans. Plasma Sci.* **34** 804–14
- [15] Morozov A I, Bugrova A I and Desyatskov A V 1997 ATON-thruster plasma accelerator *Plasma Phys. Rep.* **23** 587–97
- [16] Raitses Y and Fisch N J 2001 Parametric investigations of a nonconventional Hall thruster *Phys. Plasmas* **8** 2579–86
- [17] Courtney D G and Martinez-Sanchez M 2007 Diverging cusped-field Hall thruster (DCHT) *Proc. 30th Int. Electric Propulsion Conf. (Florence, Italy)*
- [18] Young C V, Smith A W and Cappelli M A 2009 Preliminary characterization of a diverging cusped field (DCF) thruster *Proc. 31st Int. Electric Propulsion Conf. (Ann Arbor, MI)*
- [19] Zhurin V V 2011 *Industrial Ion Sources: Broad Beam Gridless Ion Source Technology* (New York: Wiley) doi: 10.1002/9783527635726